Development of Statistical-dynamical Tools for Tropical Cyclone Intensity Prediction in the Southwest Indian Ocean. 16C.7

Marie-Dominique Leroux, Julien Meister, Dominique Mékies, Annie-Laure Dorla

16C.7

DEVELOPMENT OF STATISTICAL-DYNAMICAL TOOLS FOR TC INTENSITY PREDICTION IN THE SOUTHWEST INDIAN OCEAN

MARIE-DOMINIQUE LEROUX*
JULIEN MEISTER, DOMINIQUE MEKIES, AND ANNIE-LAURE DORLA

LACy, Laboratoire de l'Atmosphère et des Cyclones

(UMR 8105 / CNRS, Université de La Réunion, Météo-France),

Saint-Denis de La Réunion, France

1. Introduction

This research work was motivated by the lack of objective guidance tools specifically designed for the prediction of TC intensity change in the Southwest Indian Ocean (SWIO) basin. So far, in the SWIO, there was no rapid intensification (RI) definition, no formulation for the empirical maximum potential intensity (MPI), no basin-wise trained model for the prediction of TC intensity change or RI of the same ilk as DeMaria and Kaplan (1994a); Knaff et al. (2005); Knaff and Sampson (2009); Kaplan et al. (2010); Gao and Chiu (2012); Lee et al. (2015); Neetu et al. (2017); Gao et al. (2016).

Our goal is to develop similar capabilites as SHIPS (DeMaria and Kaplan 1994a) for our Regional Specialized Meteorological Center (RSMC) region of responsibility. As a key prerequisite, a 17-yr climatology was conducted to thoroughly document the SWIO tropical system activity, tracks, impacts, sizes, and 24-h intensity changes (Leroux et al. 2018); some key results are included in section 2. The dominant large-scale factors governing the intensity changes of SWIO tropical systems were then identified to provide further guidance to practical storm intensity forecasts and better anticipate rapid intensity (RI) changes. Presented here are single-lead-time versions of two models dedicated to predict storm intensity change and RI at short range over water in the SWIO.

*Corresponding author address: Météo-France DIROI, 50 boulevard du chaudron, 97491 Sainte Clotilde Cedex, La Réunion.
E-mail: marie-dominique.leroux@meteo.fr

2. Climatology of Southwest Indian Ocean Tropical Systems

The climatology was conducted using RSMC La Réunion best-track (BT) data over the geostationary satellite era (1999/2000-2015/16) that is considered homogeneous at the present time. Each year on average, 9.7 tropical systems develop in the SWIO basin, among which 9.4 are named as they strengthen into tropical storms while 4.8 systems go on to become TCs that are equivalent to a hurricane or a typhoon. This represents about 11% of global tropical system activity and almost equals the activity in the North Atlantic (NA, WMO 2017).

a. Coastal hits and threats

Fig. 1 shows that many countries in the southwest Indian Ocean are affected by tropical systems on a regular basis. On average each year, Mozambique is directly hit by one system while Madagascar, the 4^{th} biggest island on earth and one of the poorest countries in the world, is hit (threatened) by two (one) distinct system(s).

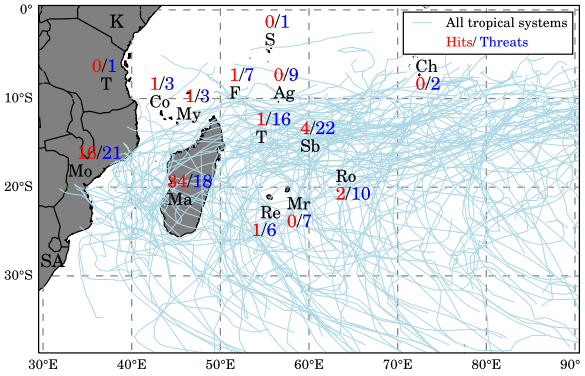

FIG. 1. Tracks of all SWIO tropical systems with a VMAX observation in the BT dataset and number of distinct tropical systems that hit (in red) or threatened (in blue) the coast of each Indian Ocean territory over the $1999-2016$ period. Any storm hitting a territory several times is only counted once. 'Hit" means that the storm center made landfall; "Threat" means that the storm center was located on the sea at less than 100 km from the coast. Letters indicate South Africa (SA), Mozambique (Mo), Tanzania (T), Kenya (K), Comoros (Co), Mayotte (My), Madagascar (Ma), Farquhar (F), Tromelin (T), Seychelles (S), La Réunion (Re), Mauritius (Mr), Agalega (Ag), Saint Brandon (Sb), Rodrigues (Ro), and the Chagos Archipelago (Ch).

b. Empirical maximum potential intensity (MPI)

The climatology of storm maximum intensity was examined by looking at the relationship between 10-

min average maximum wind speeds (VMX) from the BT dataset versus sea surface temperatures (SSTs) extracted from the OISST dataset (Reynolds et al. 2007) at storm locations during the 17-year period. The least-square fit to the maximum wind in the 22°-29°C SST range gives the empirical MPI formulation that differs from the positive exponential fit $MPI = A' + B'e^{C'(SST-T_0')}$ previously obtained in the North Atlantic (e.g., DeMaria and Kaplan 1994b; Zeng et al. 2008) and western North Pacific (Zeng et al. 2007; Gao et al. 2016).

$$MPI = \frac{A}{1 + e^{-B(SST-T_0)}} \quad (1)$$

with $A = 78.29\ \mathrm{m\,s^{-1}}$, $B = 0.3603°C^{-1}$, and $T_0 = 22.69°\mathrm{C}$. The average error between the computed MPI (Fig. 2, red curve) and the maximum wind (green curve) is $1.6\ \mathrm{m\,s^{-1}}$ over the eight SST bins ranging from 22°C to 29°C, against $2.45\ \mathrm{m\,s^{-1}}$ for a linear fit (dashed pink line).

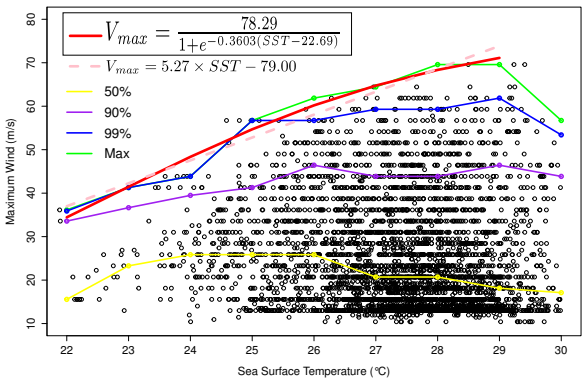

FIG. 2. Scatter diagram of maximum wind speed ($\mathrm{m\,s^{-1}}$) versus SSTs (°C) at storm locations during the $1999-2016$ period. The green, blue, purple and yellow lines respectively show the observed maximum intensity and the 99^{th}, 90^{th}, 50^{th} intensity percentiles for each 1°C SST bin. The red least-square curve is fitted to the binned maximum intensity in the $22-29°$ SST range and gives the empirical MPI formulation. The dashed pink line shows the linear fit obtained over the same SST range.

c. 24-h intensity changes (RI, RD)

The distribution of 24-h overwater intensity changes is also analyzed following the methodology previously used for the NA and eastern North Pacific systems (Kaplan and DeMaria 2003; Kaplan et al. 2010) so that comparisons can be made between basins. The two tails of the distribution give statistical definitions for rapid intensification (RI) and rapid decay (RD) in the SWIO. Based on the 94.7^{th} (4.6^{th}) percentile of 24-h intensity changes, RI (RD) can be statistically defined in the SWIO by a minimum increase (decrease) of $15.4\ \mathrm{m\,s^{-1}}$ ($13.9\ \mathrm{m\,s^{-1}}$) $\mathrm{day^{-1}}$ in the maximum surface wind speed (10-min mean). The RI threshold equals the 30-kt official threshold determined for the NA basin using 1-min sustained winds. It exceeds the $12.9\ \mathrm{m\,s^{-1}}\ \mathrm{day^{-1}}$ threshold determined for the WNP based on maximum 10-min mean winds.

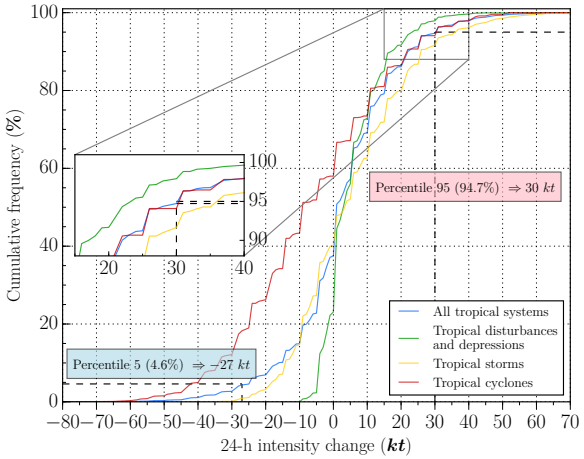

FIG. 3. Cumulative frequency distribution of overwater 24-h intensity changes (ΔV_{24} in knots, $1\ \mathrm{kt} = 0,514\ \mathrm{m\,s^{-1}}$) stratified by storm intensity at time $t = 0$ h during the $1999-2016$ period.

It is also found that a 10-min mean maximum wind speed of 65-75 kt is the most frequent initial storm intensity for RI in the SWIO (Leroux et al. 2018), consistent with the 70-80-kt peak in the maximum intensification rate of NA storms (maximum 1-min sustained wind speed; Xu and Wang 2015).

d. RSMC operational forecast errors

Statistics ran on the RSMC operational forecast errors show that, as expected, RI cases represent a challenge for intensity prediction. The mean absolute error (MAE) of intensity forecasts at short term range (within 24 h) is significantly greater for RI than non-RI cases. At 24-h lead time, $\mathrm{MAE}_{RI} = 10.8\ \mathrm{m\,s^{-1}} \gg \mathrm{MAE}_{non-RI} = 4.9\ \mathrm{m\,s^{-1}}$. This highlights the need to get additional objective forecast aids for TC intensity in the SWIO.

3. A statistical-dynamical model to predict 24-h TC intensity change

a. Data

A pool of potential predictors was examined. It includes 6 local variables extracted from the BT data at t, 20 synoptic variables extracted from ERA-Interim reanalyses along the storm-track over a 24-h period, and 8 cross-term predictors (VMX^2, MPI*VMX, MPI^2, VMX*SHR, POT^2, POT^3, DVMX12^2).

TABLE 1. List and definitions of the storm (local) and environmental (synoptic) variables with their units (1 PVU $\equiv 10^{-6}$ m^2 K s^{-1} kg^{-1}). synoptic variables are averaged over a 24-h period following t and over a disk or an annulus (as indicated in the fourth column, in km) around the storm center tracked in the corresponding ERA-Interim analyses.

Local variable	Units	Definition	
VMX	m s^{-1}	Initial maximum 10-min mean wind speed	
LAT	$^{\circ}$N	Storm center latitude	
LON	$^{\circ}$E	Storm center longitude	
SPD	m s^{-1}	Storm motion speed	
HDG	$^{\circ}$	Storm motion heading	
DVMX12	m s^{-1}	Previous 12-h wind speed change	
Synoptic variable	Units	Definition	Averaging area
SST	$^{\circ}$C	Sea surface temperature	0-200
MPI	m s^{-1}	Maximum Potential Intensity	
POT	m s^{-1}	Intensification potential: MPI - VMX	
SHR	m s^{-1}	850-200-hPa vertical wind shear	200-800
DIV200	10^{-6} s^{-1}	200-hPa divergence	200-800
DIV250	10^{-6} s^{-1}	250-hPa divergence	200-800
U200	m s^{-1}	200-hPa zonal wind	200-800
V200	m s^{-1}	200-hPa meridional wind	200-800
RHLO	%	850-700-hPa mean relative humidity	200-800
RHMD	%	700-500-hPa mean relative humidity	200-800
RHHI	%	500-300-hPa mean relative humidity	200-800
RHMID	%	700-400-hPa mean relative humidity	200-800
RV850	10^{-6} s^{-1}	850-hPa relative vorticity	0-1000
THETA	K	2-PVU potential temperature	200-800
PV200	PVU	200-hPa potential vorticity	200-800
PV300	PVU	300-hPa potential vorticity	200-800
PV400	PVU	400-hPa potential vorticity	200-800
PVT330	PVU	330-K potential vorticity	200-800
PVT350	PVU	350-K potential vorticity	200-800
PVT370	PVU	370-K potential vorticity	200-800

b. Method

A non-parametric regression technique called Multivariate adaptive regression splines (MARS Milborrow 2011) was used. It can be seen as an extension of linear models that automatically models nonlinearities and interactions between variables. The final model is built on the full sample of 18 years (1999/2000-2016/17) using 10-fold 10-cross validation, after removing 3 outliers. The optimum number of terms corresponds to the maximum mean out-of-fold R^2. The automatic variable selection is based on statistics that estimate the model generalization performance.

c. Final model

To form normalized coefficients, all of the predictors, as well as the predictand (ΔVMX_{24}) are normalized before they are incorporated in the regression equation. Subtracting the population mean and dividing this result by the population standard deviation accomplishes the normalization. The 4 predictors retained by the model are: the variation in VMX over the past 12 h (DVMX12), the mean relative humidity in the 500-300-hPa layer (RHHI), the intensification potential (POT), and the cross-term VMX*SHR. The model equation is:

$$\Delta VMX_{24} = 0.6 + \sum_{i=0}^{4} A_i * max(0, X_i - C_i) + B_i * max(C_i - X_i, 0) \quad (2)$$

with normalized coefficients listed in table 2. MARS uses hinge functions that come in pairs or not to take account non-linearities. For example, Fig. 4 shows that the tendency of the maximum wind in the next 24 h will follow that of the past 12 h but compared to previous studies, the MARS model here reverses the tendency after a 1.5 threshold of the normalized DVMX12 variable (see the kink in the predicted y), taking into account decays observed after large intensification rates or during eyewall replacement cycles.

TABLE 2. Normalized coefficients in the MARS model (equation 2).

Variable (X)	A	B	C
DVMXM12	-0.31	-0.35	1.5
RHHI	0.24	0	-1.5
POT	-0.072	-0.75	-0.66
VMX x SHR	-0.26	0	-0.8

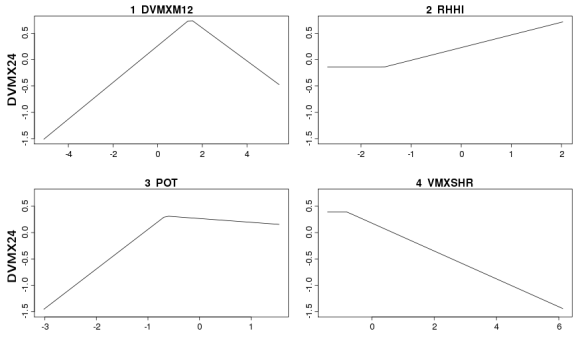

FIG. 4. Relationships between the normalized predictand (ΔVMX_{24}) and the 4 predictors in the model.

d. Model performance

The regression fit to the data explains 48% of the variance. The mean average error on the developmental data is $\text{MAE}_{train} = 4.7$ m s^{-1} versus $\text{MAE}_{train} =$ 9 kt for SH-STIPS (Knaff and Sampson 2009) and and outperforms the persistence of initial conditions with a 28% skill ($\text{MAE}_{PER} = 6.7$ m s^{-1}). The use of a multi-linear regression model yields a 5.05 m s^{-1} average error, showing that the MARS method is more skillful.

We don't have a seperate test set yet (the $2017-2018$ season) to verify the model performance against an independent dataset. Therefore, similar 18 MARS models were built on a 17-year subsample and assessed on the 18^{th} independent year. Plotted in Fig. 5 is the mean average error for each verification year. The average performance of the 18 MARS models is 5.05 m s^{-1} versus 6.7 m s^{-1} for the persistence of initial conditions which gives a model skill of 23% with a low bias of -0.12 m s^{-1}.

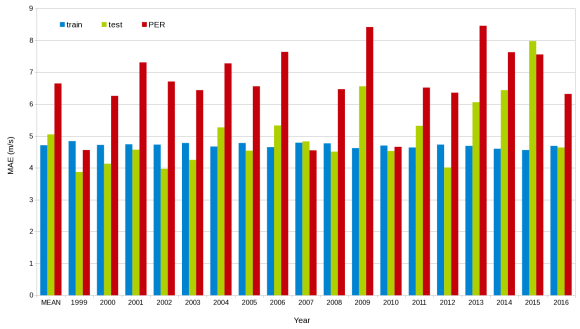

FIG. 5. MAE for the train and test data of 18 MARS models, compared to that of the persistence of initial intensity (PER).

Splitting the verification into RI and non-RI cases indicates that the MARS model is not suited to predict extreme 24-h wind changes such as RI: $\text{MAE}_{test_{RI}} =$ 13.1 m s^{-1} $\gg \text{MAE}_{test_{non-RI}} = 4.4$ m s^{-1}, hence the need of a decision tree for RI prediction.

4. TC intensity change classification for RI prediction

a. Data and Method

Our database is imbalanced because the RI cases (209) represent 5% of the population while there are 2977 non-RI cases. Therefore, the synthetic minority oversampling technique (SMOTE; Chawla (2003)) is used to oversample the cases in the RI class and avoid biased results, as in Gao et al. (2016). The 26 predictors (6 local and 20 large-scale variables) listed in Table 1 are considered.

The Classification and Regression Tree (CART, Breiman et al. 1984) is used. It is a binary decision tree that is constructed by splitting a node into two child nodes repeatedly, beginning with the root node that contains the whole learning sample. To determine the optimal number of nodes, we built 18 trees trained on 17-yr subsamples and assessed them on the 18^{th} independent year. The mean accuracy is optimized for a number of 3 nodes on average (81%).

b. Final decision tree

The final model built on the full sample of 18 years ($1999/2000$-$2016/17$) using 10-fold cross validation. Automatic variable selection is based on preset thresholds to avoid overfitting: a minimum leaf size of 100, and a complexity parameter $cp = 0.02$: any split that does not increase the overall R-squared by a factor of cp is not attempted.

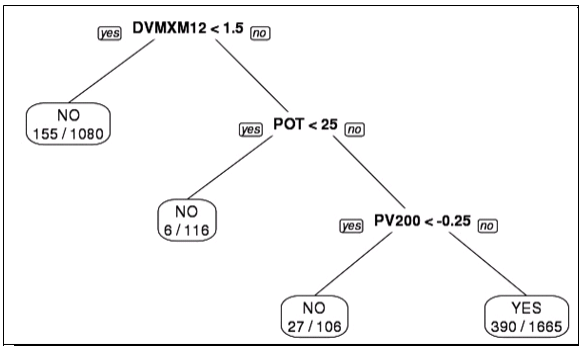

FIG. 6. The decision tree for the prediction of RI (class labeled YES) at 24-h lead time constructed from the potential predictors in Table 1. Also shown are the number of misclassified samples / the total number of samples from both classes fulfilling the conditions of each tree path.

Fig. 6 shows 3 rules. Rule 1 states that RI generally will not happen if the wind increase in the past 12 h is lower than 1.5 m s^{-1}. Rule 2 states that if the wind increase in the past 12 h is higher than 1.5 m s^{-1} but the POT is lower than 25 m s^{-1} then a TC will not rapidly intensify. Rule 3 adds a third condition for RI to happen: the PV at 200 hPa in the environment of the TC must be close to neutral or not too cyclonic (i.e. there must not be a Rossby wave breaking event associated with possible shear nearby).

c. Model evaluation

The prediction accuracy of the model is 81% (Table 3), with a high probability of dectection (POD $= 1275/1463 = 87\%$) and a low false alarme rate

(FAR $= 390/1665 = 23\%$). We did not run an independent verification yet.

TABLE 3. Confusion matrix from 10-fold cross validation of the decision tree shown in Fig. 6.

		Classified		Total
		RI	non-RI	
Observed	RI	1275	188	1463
	non-RI	390	1114	1504
Total		1665	1302	**2967**

Summary & **future plans**

A 17-year climatology of tropical system activity, tracks, impacts, sizes, and 24-h intensity changes was produced in an effort to thoroughly document the southwest Indian Ocean and provide further guidance to practical storm intensity forecasts. A first formulation of the empirical maximum potential intensity of SWIO tropical systems was derived. Based on the examination of a total of 26 potential predictors (including the MPI), statistical-dynamical tools of the same ilk as those developed in other basins have been designed to predict TC intensity change or RI at short range. The single-lead-time versions of the two models look suitable as operational TC intensity forecast tools for use at RSMC La Réunion and will be tested over the next TC seasons to assess their actual real-time performance. A degradation of the performance is expected since the models were built using a perfect prognosis approach (with BT data and reanalyses). In real-time, the ECMWF model forecast fields will be used to derive the large-scale environmental predictors along the RSMC TC track forecast, which includes additional sources of intensity forecast errors not accounted for in the developmental data. In the near future, we will investigate the need to develop prediction models for other lead-times and the relevance of deriving a MARS regression model based on only RI cases (which should highlight different key predictors).

REFERENCES

Breiman, L., J. Friedman, R. Olshen, and C. J. Stone, 1984: Classification and Regression Tree. Cole Advanced Books & Software, Pacific California.

Chawla, N. V., 2003: C4.5 and imbalanced data sets: Investigating the effect of sampling method, probabilistic estimate, and decision tree structure. *Proc. Int. Conf. on Machine Learning*, Washington, DC, International Machine Learning Society, [Available online at https://www3.nd.edu/;dial/papers/ICML03.pdf.

DeMaria, M. and J. Kaplan, 1994a: A Statistical Hurricane Intensity Prediction Scheme (SHIPS) for the Atlantic Basin. *Wea. Forecasting*, **9**, 209–220.

DeMaria, M. and J. Kaplan, 1994b: Sea surface temperature and the maximum intensity of Atlantic tropical cyclones. *J. Climate*, **7**, 1324–1334.

Gao, S. and L. S. Chiu, 2012: Development of statistical typhoon intensity prediction: Application to satellite observed surface evaporation and rain rate (STIPER). *Wea. Forecasting*, **27**, 240–250.

Gao, S., W. Zhang, J. Liu, I.-I. Lin, L. S. Chiu, and K. Cao, 2016: Improvements in Typhoon Intensity Change Classification by Incorporating an Ocean Coupling Potential Intensity Index into Decision Trees. *Wea. Forecasting*, **31**, 95–106.

Kaplan, J. and M. DeMaria, 2003: Large-scale characteristics of rapidly intensifying tropical cyclones in the North Atlantic basin. *Wea. Forecast.*, **18**, 1093–1108.

Kaplan, J., M. DeMaria, and J. A. Knaff, 2010: A revised tropical cyclone rapid intensification index for the Atlantic and eastern North Pacific basins. *Wea. Forecasting*, **25**, 220–241.

Knaff, J. A. and C. R. Sampson, 2009: Southern hemisphere tropical cyclone intensity forecast methods used at the Joint Typhoon Warning Center, Part II: forecasts based on a statistical-dynamical approach. *Aust. Meteor. and Oceanogr. J.*, **58**, 9–18.

Knaff, J. A., C. R. Sampson, and M. DeMaria, 2005: An operational Statistical Typhoon Intensity Prediction Scheme for the western North Pacific. *Wea. Forecasting*, **20**, 688–699.

Lee, C.-Y., M. K. Tippett, S. J. Camargo, and A. H. Sobel, 2015: Probabilistic Multiple Linear Regression Modeling for Tropical Cyclone Intensity. *Mon. Wea. Rev.*, **143**, 933–954.

Leroux, M.-D., J. Meister, D. Mekies, A.-L. Dorla, and P. Caroff, 2018: A climatology of southwest indian ocean tropical systems: Their number, tracks, impacts, sizes, empirical maximum potential intensity, and intensity changes. *Journal of Applied Meteorology and Climatology*, **57 (4)**, 1021–1041, doi:10.1175/JAMC-

D-17-0094.1, URL https://doi.org/10.1175/JAMC-D-17-0094.1, https://doi.org/10.1175/JAMC-D-17-0094.1.

Milborrow, S., 2011: *earth: Multivariate Adaptive Regression Splines*. URL https://CRAN.R-project.org/package=earth, r package.

Neetu, S., et al., 2017: Global assessment of tropical cyclone intensity statistical-dynamical hindcasts. **143**, 2143–2156.

Reynolds, R. W., T. M. Smith, C. Liu, D. B. Chelton, K. S. Casey, and M. G. Schlax, 2007: Daily high-resolution-blended analyses for sea surface temperature. *J. Climate*, **20**, 5473–5496.

WMO, 2017: Global Guide to Tropical Cyclone Forecasting. World Meteorological Organization, WMO/TD-No. 1194, Geneva, URL http://www.wmo.int/cycloneguide/pdf/Global-Guide-to-Tropical-Cyclone-Forecasting.pdf.

Zeng, Z.-H., L.-S. Chen, and Y. Wang, 2008: An Observational Study of Environmental Dynamical Control of Tropical Cyclone Intensity in the Atlantic. *Mon. Wea. Rev.*, **136**, 3307–3322.

Zeng, Z.-H., Y. Wang, and C.-C. Wu, 2007: Environmental dynamical control of tropical cyclone intensity – An observational study. *Mon. Wea. Rev.*, **135**, 38–59.